Commun. Comput. Phys.
doi: 10.4208/cicp.381011.270112s

Vol. **13**, No. 3, pp. 649-670
March 2013

On Triangular Lattice Boltzmann Schemes for Scalar Problems

François Dubois[1,*] and Pierre Lallemand[2]

[1] *Conservatoire National des Arts et Métiers, Department of Mathematics, Paris*, and *Department of Mathematics, University Paris-Sud, Bât. 425, F-91405 Orsay Cedex, France.*
[2] *Centre National de la Recherche Scientifique, Paris, France.*

Received 31 October 2011; Accepted (in revised version) 27 January 2012

Available online 29 August 2012

Abstract. We propose to extend the d'Humières version of the lattice Boltzmann scheme to triangular meshes. We use Bravais lattices or more general lattices with the property that the degree of each internal vertex is supposed to be constant. On such meshes, it is possible to define the lattice Boltzmann scheme as a discrete particle method, without need of finite volume formulation or Delaunay-Voronoi hypothesis for the lattice. We test this idea for the heat equation and perform an asymptotic analysis with the Taylor expansion method for two schemes named D2T4 and D2T7. The results show a convergence up to second order accuracy and set new questions concerning a possible super-convergence.

AMS subject classifications: 65-05, 65Q99, 82C20

Key words: Laplacian operator, heat equation, d'Humières scheme, D2T4, D2T7.

1 Introduction

The importance of extending the lattice Boltzmann scheme from square type regular meshes to unstructured triangulations has been recognized during the last years of 20th century [5, 22, 29]. In particular the "volumetric formulation" of Chen [5] makes a link with finite volumes, using control volumes around each vertex (the "Inria cells" [41]) of a finite element type triangulation. This method is still under active development with the work of Succi, Ubertini and co-workers [30, 35, 36]. In a dual way, van der Sman [37–40] uses rectangles and triangles as control volumes with a "cell center" type approach in Roache [33] denomination. He has developed an approximation of diffusion equation with Delaunay-Voronoi meshes for a BGK variant of the lattice Boltzmann scheme.

*Corresponding author. *Email address:* francois.dubois@math.u-psud.fr (F. Dubois)

In a previous contribution [12], we have observed that for usual lattice Boltzmann schemes (as for example the well known D2Q9), several (two for D2Q9) families of finite volumes are naturally associated with the scheme. As a consequence, we consider now the lattice Boltzmann scheme essentially as a "particle" method on a given (*a priori* fixed) mesh with discrete velocities. Recall that the "Particle In Cell" method has been first proposed in 1964 by Harlow *et al.* [18] and has been analyzed in the eighties by Beale and Majda [2], Raviart, Cottet and Mas Gallic [8, 28, 32] among others. We remark that this particle method does not suppose *a priori* the existence of a given lattice. The surrounding cells are recomputed at each time step in order to make the particle interact. Dynamic triangulation is an alternative to the previous methodology. It has been developed recently by Cianci, Klales, Love and co-workers [23, 26] in the context of lattice gas automata.

In this contribution, instead of adopting the volumetric formulation or a Delaunay-Voronoi hypothesis, we develop the framework of lattice Boltzmann schemes as a variant of the particle method. We propose an extension of the approach of d'Humières [9] to triangular meshes and we restrict this first tentative to scalar problems like the heat equation without advection.

The outline of the contribution is the following. We first recall the classic D2T7 lattice Boltzmann scheme in the next section. At this occasion, we put in evidence a property of symmetry of Bravais lattices. It is possible to adapt the Taylor expansion analysis [10] to this triangular lattice, with a diffusive scaling. This development is presented in Section 3 and applied to the D2T7 scheme. Several simulations with the D2T7 lattice Boltzmann scheme for the heat equation are presented in Section 4. In Section 5, we set the question of defining a discrete particle method on a finite element type triangular lattice. We propose a partial answer when each vertex of the lattice has a constant number of neighbours. This framework is applied in Section 6 to define a D2T4 lattice Boltzmann scheme for the heat equation. We repeat in Section 7 with this new scheme "D2T4" the simulations presented in Section 4. This work validates the potential of applications of our proposal. The conclusion (section 8) serves also as a discussion concerning encountered difficulties.

2 D2T7 lattice Boltzmann scheme

We consider a Bravais lattice $\mathcal{L}$ connecting nodes labelled by the letter x and parametrized by a typical space scale Δx. The neighbour vertex number j of the node $x \in \mathcal{L}$ is denoted by x_j and we set

$$x_j = x + \xi_j \Delta x. \tag{2.1}$$

For each $x \in \mathcal{L}$ and each direction ξ_j linking two vertices, the "opposite node" with number $\sigma(j)$ defined according to

$$x_{\sigma(j)} \equiv x - \xi_j \Delta x, \qquad \xi_j + \xi_{\sigma(j)} \equiv 0 \tag{2.2}$$

is also a vertex of the lattice $\mathcal{L}$ (*i.e.* $x_{\sigma(j)} \in \mathcal{L}$). In the following, we emphasize this property satisfied by Bravais lattices and qualify it as a symmetric property. Most "DdQq" schemes (with a notation introduced by Qian *et al.* [31]) presented in the literature use a Bravais lattice. This symmetry property is also mandatory *e.g.* to define "two relaxation times" lattice Boltzmann schemes as proposed by Ginzburg *et al.* [16].

The lattice Boltzmann scheme with multiple relaxation times is defined in a classical manner. Consider a vertex x that belongs to the lattice $\mathcal{L}$. Then the j^{o} direction of propagation is defined with a vector ξ_j and $\xi_j \in \mathcal{V}$, set of directions that define the vicinity of the vertex x. The j^{o} density of particles at vertex x and time t is denoted by $f_j(x,t)$. After a local step of relaxation, the j^{o} density of particles is named $f_j^*(x,t)$. Because a Bravais lattice $\mathcal{L}$ is symmetric, the neighbouring vertex $x_{\sigma(j)}$ defined in (2.2) in the direction **opposite** to the j^{o} direction of propagation belongs to the lattice $\mathcal{L}$. The lattice Boltzmann scheme can be completely defined:

$$f_j(x,t+\Delta t) = f_j^*(x-\xi_j \Delta x, t). \tag{2.3}$$

Moreover the basic iteration (2.3) of a lattice Boltzmann scheme supposes explicitly that the lattice is symmetric, as illustrated in Fig. 1 (left).

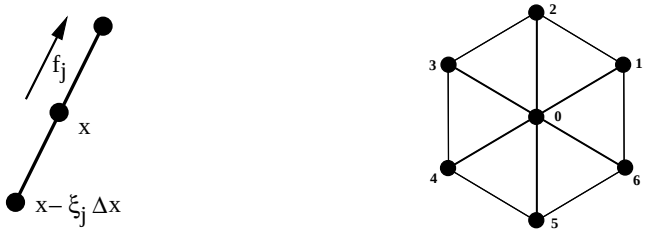

Figure 1: Typical stencil of a lattice Boltzmann scheme for a Bravais lattice (left) ; both opposite directions ξ_j and $-\xi_j$ connect two vertices of the mesh. Local numbering of the six neighbours (right) of the D2T7 lattice Boltzmann scheme on triangles.

The D2T7 lattice Boltzmann uses equilateral triangles as suggested by Frisch, Hasslacher and Pomeau in 1986 [14] in the context of lattice gas automata. We precise the parameters that we have to consider. A vertex x has a total of six neighbours (seven including itself) ξ_j $(j=0,\cdots,6)$ as in Fig. 1 (right). Following d'Humières approach [9] we introduce moments m_k as linear functions of the particle distribution f:

$$m_k = \sum_j M_{kj} f_j. \tag{2.4}$$

We restrict our study to the simple case of only one conservation (thermal problem). Following [24], we introduce a family $\mathcal{P}$ of polynomials p_k for $k=0,\cdots,6$:

$$\mathcal{P} = \left\{1, X, Y, X^2+Y^2, \frac{4}{\sqrt{3}}XY, 2(X^2-Y^2), 3Y-4Y^3\right\}. \tag{2.5}$$

The coefficients of the matrix M introduced at relation (2.4) are simply given by a nodal value in the velocity space:

$$M_{kj}=p_k(\xi_j),\qquad 0\leq j,k\leq 6. \tag{2.6}$$

We remark that $M_{\alpha j}=\xi_j^\alpha$ for $\alpha=1,2$. We have only one conserved moment $\rho\equiv m_0=m_0^{\rm eq}=m_0^*=\sum_j f_j$ and the other moments at equilibrium follow the relations $m_1^{\rm eq}=m_2^{\rm eq}=0$, $m_3^{\rm eq}=a_3\rho$, $m_4^{\rm eq}=m_5^{\rm eq}=m_6^{\rm eq}=0$. The relaxation of moments out of equilibrium is also very simple:

$$m_k^*=m_k+s_k(m_k^{\rm eq}-m_k),\qquad k=1,\cdots,6, \tag{2.7}$$

with $s_1=s_2$ and $s_4=s_5$ to enforce isotropy.

3 Taylor expansion with diffusive scaling

We can analyse the D2T7 lattice Boltzmann scheme with the Taylor expansion method [10]. We consider one time step of iteration (2.3) and we replace the particle distribution in the right hand side by the moments after relaxation:

$$f_j(x,t+\Delta t)=\sum_\ell M_{j\ell}^{-1}m_\ell^*(x-\xi_j\Delta x,t). \tag{3.1}$$

In consequence, we have the formal expansion in the moment space

$$\begin{aligned} m_k(x,t+\Delta t)&=\sum_{j\ell}M_{kj}M_{j\ell}^{-1}\,m_\ell^*(x-\xi_j\Delta x,t)\\ &=\sum_{j\ell}M_{kj}M_{j\ell}^{-1}\left[m_\ell^*(x,t)-\xi_j^\alpha\,\Delta x\partial_\alpha m_\ell^*+\mathcal{O}(\Delta x^2)\right]\\ &=m_k^*-\Delta x\sum_\ell\Big(\sum_j M_{kj}\,\xi_j^\alpha\,M_{j\ell}^{-1}\Big)\,\partial_\alpha m_\ell^*+\mathcal{O}(\Delta x^2). \end{aligned} \tag{3.2}$$

We introduced the momentum-velocity tensor introduced in [10]: $\Lambda_{kp}^\ell\equiv\sum_j M_{kj}\,M_{pj}\,M_{j\ell}^{-1}$. Then we have up to third order accuracy

$$m_k(x,t+\Delta t)=m_k^*-\Delta x\,\Lambda_{k\alpha}^\ell\,\partial_\alpha m_\ell^*+\frac{1}{2}\Delta x^2\,\Lambda_{k\alpha}^p\,\Lambda_{p\beta}^\ell\,\partial_\alpha\partial_\beta m_\ell^*+\mathcal{O}(\Delta x^3)$$

and using the relaxation step (2.7),

$$m_k^*(x,t+\Delta t)=m_k^{\rm eq}-\Delta x\,\frac{1-s_k}{s_k}\,\Lambda_{k\alpha}^\ell\,\partial_\alpha m_\ell^{\rm eq}+\mathcal{O}(\Delta x^2).$$

We adopt the so-called "diffusive scaling" proposed initially for rarefied flows by Sone [34] (see an explicit derivation for lattice Boltzmann schemes *e.g.* in Junk *et al.* [20])

$$\Delta t\equiv\frac{\Delta x^2}{\zeta}, \tag{3.3}$$

where ζ is a constant for homogeneity of dimensions. We add some advection term by enforcing the relations according to $m_1^{\rm eq}=u\frac{\Delta x}{\zeta}$ and $m_2^{\rm eq}=v\frac{\Delta x}{\zeta}$. After some pages of formal calculus, following the method presented in details in [13], we obtain the equivalent partial differential equation :

$$\frac{\partial\rho}{\partial t}+u\frac{\partial\rho}{\partial x}+v\frac{\partial\rho}{\partial x}-\mu\Delta\rho=\Theta\Delta x^2\,\Delta^2\rho+\Delta x^4\,A_6\rho+\mathcal{O}(\Delta x^6). \tag{3.4}$$

Up to second order accuracy, we have an approximation of the heat equation with a diffusivity coefficient μ given according to

$$\mu=\frac{1}{2}\zeta a_3\sigma_1.$$

The coefficients σ_k for the nonconserved moments are given by the Hénon's relation [19] $\sigma_k\equiv\frac{1}{s_k}-\frac{1}{2}$. The coefficient Θ in front of the fourth order term in (3.4) is explicited as follows for $u=v=0$:

$$\Theta=-\frac{1}{16}\sigma_1 a_3\zeta\Big((1-a_3)\,(1-4\sigma_1\sigma_3)-2\sigma_1\sigma_4+4a_3\sigma_1^2\Big). \tag{3.5}$$

In the relation (3.4), A_6 is a sixth order operator. The development of the other moments can also be achieved. In particular, we have $m_\alpha=m_\alpha^{\rm eq}-\frac{a_3}{2s_1}\Delta x\partial_\alpha\rho+\mathcal{O}(\Delta x^2)$.

"Second order", "quartic" and "hexahedric" coefficients

We have chosen the following numerical values $\zeta=1, a_3=\frac{1}{4}, s_1=0.8$ compatible with a diffusivity coefficient μ=0.09375. In these conditions, the D2T7 lattice Boltzmann scheme is formally equivalent to the heat equation up to order 2 (*id est*, due to (3.4) and (3.5), $\Theta\neq0$ and $A_6\neq0$) when using to fix the ideas the following "second order" coefficients (given here with 15 decimals for a possible implementation):

$$s_3=1.428571428571428,\quad s_4=s_5=0.481927710843373,\quad s_6=0.476190476190476. \tag{3.6}$$

With the following choice of "quartic" relaxation coefficients

$$s_3=1.428571428571428,\quad s_4=s_5=0.930232558139534,\quad s_6=0.526315789473684, \tag{3.7}$$

the D2T7 lattice Boltzmann scheme is formally of the order 4 (*id est* $\Theta=0$ and $A_6\neq0$). Last but not least, we can impose $\Theta\equiv0$ and $A_6\equiv0$ and the D2T7 scheme is of order 6. The "hexahedric" coefficients can be taken as follows:

$$s_3=1.086117521785847,\quad s_4=s_5=1.344205296559553,\quad s_6=0.647305233773416. \tag{3.8}$$

4 Diffusion simulations with the D2T7 scheme

We have done several simulations: a "one point" periodic analysis, a numerical evaluation of the modes for a periodic pipe and a rectangle, the computation of harmonic functions by time asymptotics of the heat equation, the dissipation of a triangular Dirichlet mode and the direct numerical computation of triangular Dirichlet modes.

One point periodic analysis

The one point analysis can be conducted as follows. We start from the iteration (2.3) of a lattice Boltzmann scheme. We suppose that the particle field for the neighbouring points of vertex x satisfy the following periodicity condition:

$$f_j\big(x-\xi_j\Delta x,t\big)=\exp\big(-i\mathbf{k}\bullet\xi_j\Delta x\big)\,f_j\big(x,t\big) \tag{4.1}$$

for some wave vector $\mathbf{k}=(k\cos\theta,k\sin\theta)$. From (4.1), the evaluation of the right hand side of (2.3) is easy in the context of the d'Humières version of the lattice Boltzmann scheme. The state vector f is then solution of an eigenvalue problem of small dimension q for a general lattice Boltzmann problem with q velocities. In the D2T7 case for thermal problems, we obtain six eigenvalues $\lambda_\ell\simeq 1-s_\ell$ for $\ell\geq 1$ and one physical eigenvalue $\lambda(\mathbf{k})\simeq 1-\mu k^2$. This eigenvalue has a real meaning for applications to macroscopic physics. A numerical diffusivity $\mu_{\rm num}\equiv(1-\lambda(\mathbf{k}))/k^2$ can be extracted from the previous relation. In Fig. 2, we have plotted the error $\epsilon\equiv|\,\mu-\mu_{\rm num}\,|$ as a function of the modulus of the wave vector. With the three versions of the D2T7 scheme detailed in (3.6), (3.7) and (3.8), the errors for the diffusivity have an order of convergence directly predicted by the Taylor expansion analysis.

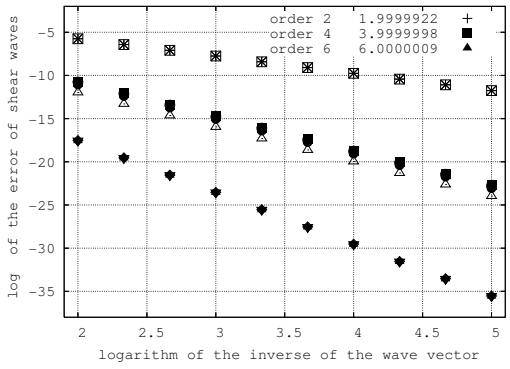

Figure 2: D2T7 lattice Boltzmann scheme for the heat equation. One point periodic analysis. Error $\epsilon\equiv|\mu-\mu_{\rm num}|$ between exact and numerical diffusivities. Note that the exact dispersion equation can be obtained, and when solved by successive approximations in powers of k, it leads to the same results, obtained from the successive equivalent equations.

Periodic pipe and rectangle

The analysis for a periodic pipe is conducted by following the same ideas. A D2T7 lattice Boltzmann solver is considered on a simple geometry of $nx \equiv 96$ by $ny \equiv 4$ mesh points. The unknown is now a vector $f \in \mathbb{R}^{7nxny}$. The iteration of the scheme defines a linear operator A and the first eigenvalue of this operator is determined thanks to an Arnoldi algorithm [1]. The first eigenvalue $\lambda \equiv 1$ corresponds to the conservation of mass in the whole domain, including boundary conditions. The second eigenvalue λ_0 corresponds to the smallest wave vector compatible with the computational domain. It is compared with the modulus of the wave vector to evaluate a numerical diffusivity $\mu_{\rm num} = (1-\lambda_0)/k^2$ as previously. The different errors $\epsilon \equiv |\mu - \mu_{\rm num}|$ are presented in Fig. 3 (left). The first two versions (3.6)-(3.7) of orders two and four present a coherent numerical convergence. The results are not so clear with the sixth order tuning of the parameters. It seems to be due to the round-off errors for this study involving three orders of magnitude for wave vector.

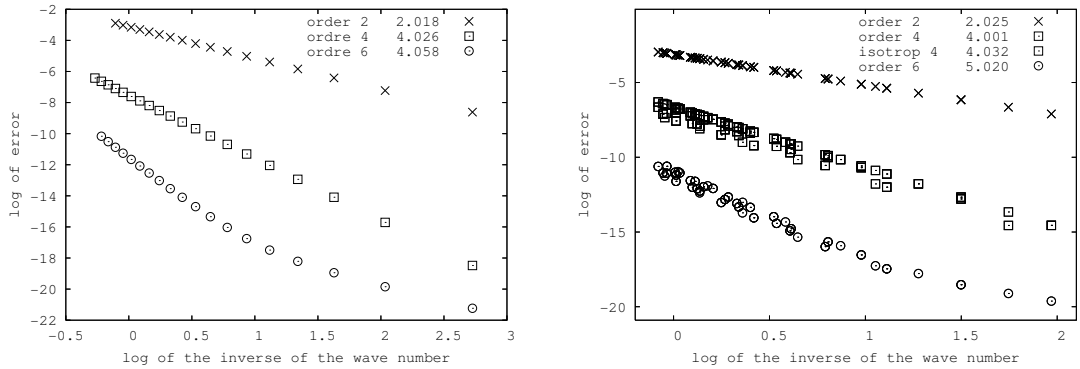

Figure 3: D2T7 lattice Boltzmann scheme for the heat equation. Periodic modes for a pipe with $nx = 96$ and $ny = 4$ mesh points (left) an periodic modes for a rectangle of $nx = 36$ by $ny = 52$ points (right). Error $\epsilon \equiv |\mu - \mu_{\rm num}|$ between exact and numerical diffusivities. The hexahedric predicted coefficients define a fourth or fifth order scheme.

The analysis is analogous for a rectangle $nx \equiv 36$ by $ny \equiv 52$ mesh points. The results are depicted in Fig. 3 (right). The lattice Boltzmann scheme has a coherent order of convergence for the "second order" and "fourth order" versions of the scheme. The "sixth order" scheme exhibits now an error numerically evaluated as only fifth order accurate. This fact seems again to due to round-off errors in the Arnoldi process [1].

Harmonic polynomials on a triangle

We have developed a D2T7 solver for a triangular geometry (see a typical mesh in Fig. 4) The initial condition is *a priori* identically null. We determine the numerical boundary conditions compatible with a polynomial expression $p_H(x,y) \equiv x^2 - y^2$ on the boundary with an "anti-bounce-back" version of the algorithm of Bouzidi *et al.* [3]. The computation converges in time towards the harmonic function introduced above. We present in

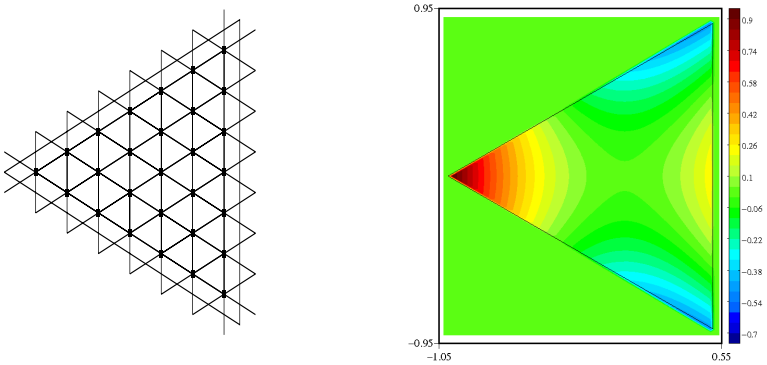

Figure 4: Typical two-dimensional mesh for a D2T7 computation on a triangle (left). Two-dimensional computation of the harmonic function $p_H(x,y)=x^2-y^2$ on a triangle with the D2T7 lattice Boltzmann scheme (right). The iso-contours are composed by discrete hyperbolas.

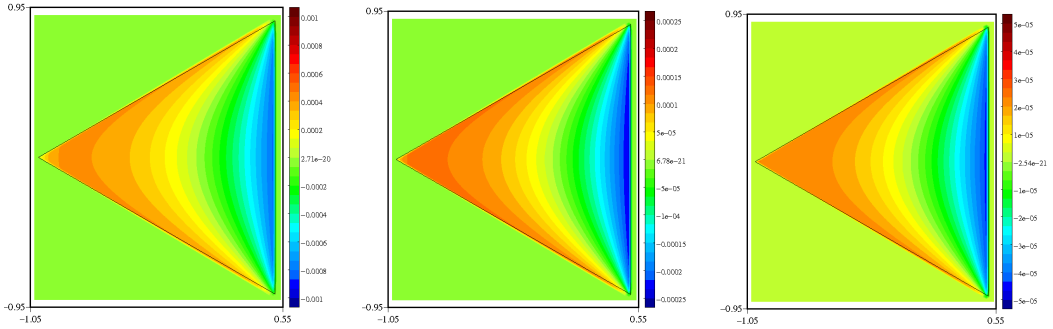

Figure 5: Two-dimensional computation of the harmonic function $p_H(x,y)=x^2-y^2$ on a triangle with the D2T7 lattice Boltzmann scheme. Iso-contours of the errors for three sets of parameters presented at relations (3.6), (3.7) and (3.8). Negative values are in blue and positive ones in red. The maximal errors are equal to 8.1410^{-4} (left), 2.3610^{-4} (middle) and 4.4710^{-5} (right) when using a D2T7 scheme with formal order of 2 (left), 4 (middle) and 6 (right).

Fig. 4 (right) the numerical result $\rho(x,y)\simeq p_H(x,y)$ when we use 61 points on the edge of the triangle (that corresponds to a total of 1891 vertices for the entire mesh).

In Fig. 5, we have plotted the error field for the three versions (3.6), (3.7), (3.8) of the D2T7 lattice Boltzmann scheme. The results are qualitatively coherent: the more the scheme is theoretically precise, the more the error is reduced. In Fig. 6 (left), we observe that the L^∞ error is substantially reduced when the parameters induce a better precision. But the order of convergence remains very close to second order even for "fourth order" and "sixth order" versions of the scheme using the set of parameters (3.7) or (3.8). In this case this default can be due to a possible deficit of time steps and to crude boundary conditions. The lattice Boltzmann scheme is explicit and the time iterations (see Fig. 6, right) take too much time to reach convergence to the stationary state with a satisfactory reduction of the error.

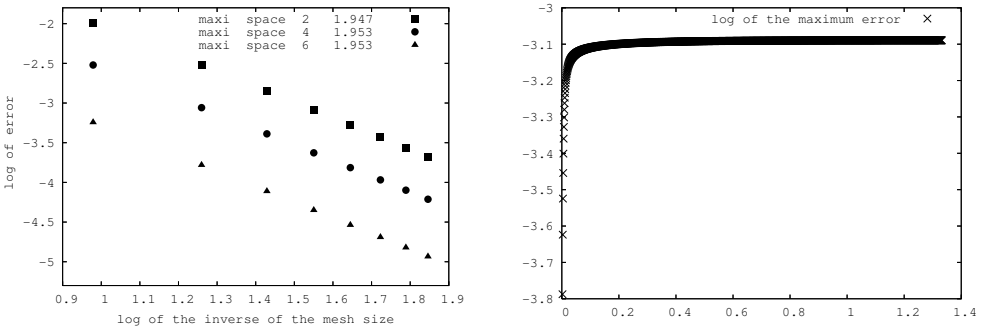

Figure 6: Two-dimensional computation of the harmonic function $p_H(x,y)=x^2-y^2$ on a triangle with the D2T7 lattice Boltzmann scheme. No extra order is observed for the L^∞ error when refining the mesh (left). The evolution in time is very slow (right), even initializing the computation with the exact solution!

Dissipation of a triangular Dirichlet mode

We have also experimented the relaxation of a Dirichlet mode. The first mode is simply a product of three "sinus" functions, as first explicited by Lamé (see McCartin [27]). With our nomenclature, the eigenvalue number ℓ is proportional to $3(\ell-1)^2$. The reference value is in consequence equal to 12, 48 and 108 for ℓ equal to 3, 5 and 7 respectively. We present in Fig. 7 the results at $T=4/3$ and the evolution of the physical field at the center. The asymptotic analysis obtained by successive mesh refinements is presented in Fig. 8. We measure the error in time for the center vertex as the mesh size tends to zero and the L^∞ error at the precise time $T=4/3$ in the same conditions. The results are correct but not easy to interpret. The "second order" scheme is just a bit better that the order $3/2$. The "fourth order" version is of order 3 and the "sixth order" scheme hesitates between the orders 3 and 4.

Dirichlet modes for a triangle

We used the D2T7 lattice Boltzmann scheme (2.3) to define a linear operator $f(t)\longmapsto f(t+\Delta t)\equiv A\bullet f(t)$ where $f(t)$ is the vector of all unknowns for the entire mesh. Then the first eigenvalues of the linear operator A are computed with the Arnoldi algorithm [1].

Some exact reference modes are displayed in the left part of Figs. 9-11. The numerical approximation is globally of very good quality and we have plotted the errors for different modes computed on the same lattice in the same figures. We perform the computations for each mode, one with the "second order" accurate version of the D2T7 scheme and the other one with a "fourth order" accurate tuning of numerical parameters. In each case, we compare the theoretical eigenvalue after applying a suitable normalization and the computed eigenvalue by the Arnoldi algorithm. The results are of good quality and the quartic parameters give a better precision for the numerical results. Even if the fourth order convergence is not established, the tuning of parameters improves clearly the numerical quality.

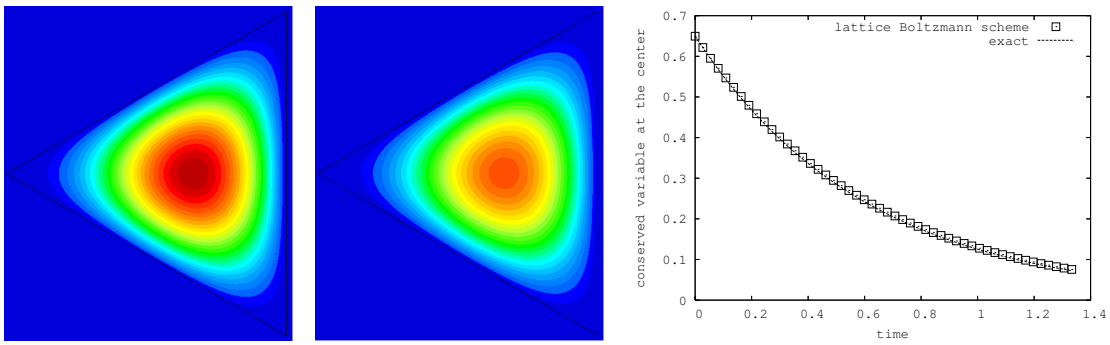

Figure 7: Isovalues of the first Dirichlet mode for an equilateral triangle (left). Dissipation of this mode by time evolution: D2T7 solution at time $T=4/3$ for 76 points on the edge (2926 vertices, middle). Exponential decay at the center of the mesh (55 vertices, right).

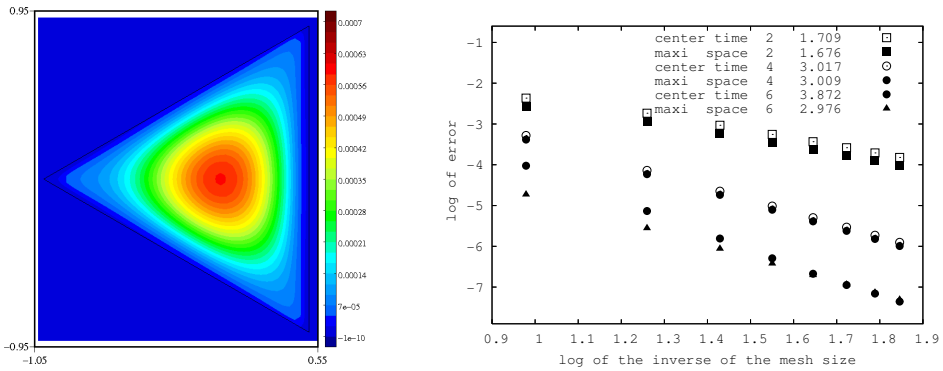

Figure 8: Dissipation of the first Dirichlet mode. Isocontours of the field of error at $T=4/3$ with a mesh composed by 61 points on the edge (left). Negative values in blue and positive ones in red. Time and L^∞ space errors for several meshes and several "orders" with the D2T7 lattice Boltzmann scheme. The obtained accuracy is not the one proposed by the Taylor expansion method. The space numerical accuracy is going from 1.7 to 3.0 with a good tuning of the numerical parameters.

5 Lattice Boltzmann scheme on arbitrary meshes?

Imagine that we move the vertices in the Bravais lattice presented at Fig. 4 (left). We obtain a topologically regular mesh in the sense that the number of edges containing a given internal vertex is constant. An example is proposed at Fig. 12. This mesh is a good candidate for future extensions of the lattice Boltzmann scheme. With this kind of classical finite element type mesh, it is possible to use all the engineering tools of automatic meshing in two and three space dimensions as described *e.g.* in [15]. But this goal is still not the purpose of the present contribution. The vertices of the mesh of Fig. 12 are now the nodes of a cellular complex and each vertex has a **constant** number of neighbours. In other terms, the degree of each vertex is constant. We denote by $x_j \equiv x+\xi_j(x)\Delta x$ the vertex belonging to the lattice $\mathcal{L}$ with a local neighbouring number j relative to the vertex x. Remark that the vertex x is also a neighbour of the vertex x_j with

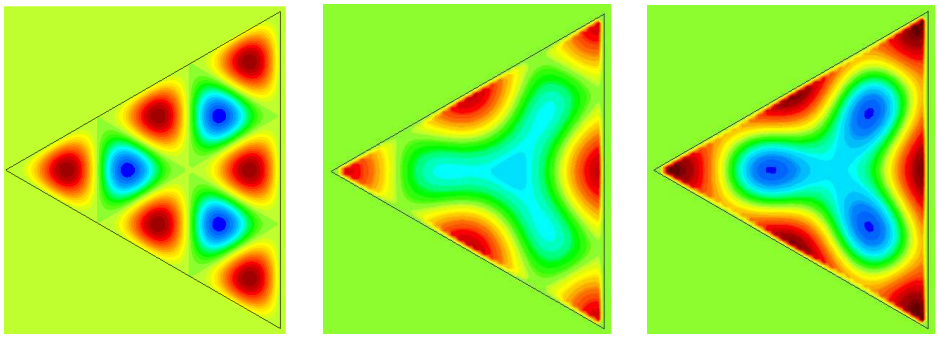

Figure 9: Isovalues of the Dirichlet mode number "3" of an equilateral triangle (left) and errors for a D2T7 computation. The exact reference eigenvalue is equal to 12 (in appropriate units). The numerical eigenvalue is equal to 11.99902 with second order parameters (middle) and to 11.99938 with "fourth order" parameters (right). The L^∞ error for the modes is equal to 4×10^{-4} at order 2 and 10^{-4} at order 4. The figures show the isovalues of the error for both computations with different scales. We observe that the global shape of these errors is similar to isovalues of the reference eigenvector.

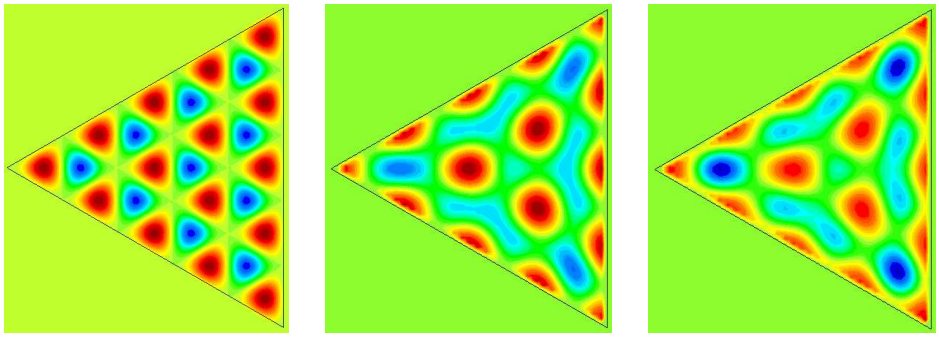

Figure 10: Isovalues of the Dirichlet mode number "5" of an equilateral triangle (left) and errors for a D2T7 computation. The exact reference eigenvalue is equal to 48. The numerical eigenvalue is equal to 47.98339 at order 2 (middle) and to 47.98842 at order 4 (right). The L^∞ error for the modes is equal to 3×10^{-2} at order 2 and 1.1×10^{-3} at order 4.

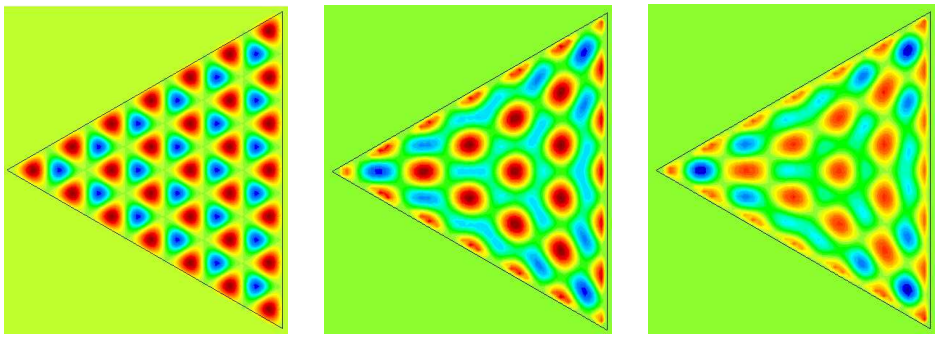

Figure 11: Dirichlet mode number "7" of an equilateral triangle (left) and errors for a D2T7 computation. The exact reference eigenvalue is equal to 108. The numerical eigenvalue is equal to 107.90777 at order 2 (middle) and to 107.92705 at order 4 (right). The L^∞ error for the modes with this computation is equal to 1.02×10^{-2} at order 2 and 4.2×10^{-3} at order 4.

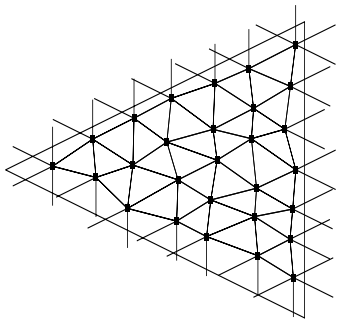

Figure 12: Triangular lattice obtained from a little random displacement of the vertices of an equilateral triangular mesh.

a local number $\ell \equiv n_j(x)$. We have the obvious relation $\xi_j(x)+\xi_\ell(x_j) \equiv 0$ and in other terms the identity

$$\xi_j(x)+\xi_{n_j(x)}(x_j) \equiv 0. \tag{5.1}$$

As previously, we denote by $f_j(x)$ the density of particles going from vertex x towards vertex x_j. Moreover, the outgoing particles from vertex x_j are also ingoing particles "into" vertex x with an index denoted by ℓ.

We precise the previous notation. If $f_j(x)$ is the density of particles from the vertex x towards the vertex x_j, $f_j^*(x)$ denotes the same quantity **after relaxation**. In a dual vision, we denote by $f_\ell^*(x_j)$ the density of particles going from the vertex x_j in the direction of the vertex x after relaxation. We have also to consider the density $\widetilde{f}_j(x)$ of particles going from the vertex x_j towards the vertex x. The lattice Boltzmann scheme is a particle method. The flight of particles between the vertex x_j and the vertex x takes exactly one time step : $\widetilde{f}_j(x,t+\Delta t) = f_\ell^*(x_j,t)$. If we replace the notation ℓ for the index of vertex x relative to its neighbour x_j by the notation $n_j(x)$ introduced previously at relation (5.1), the lattice Boltzmann scheme takes the form

$$\widetilde{f}_j(x,t+\Delta t) = f_{n_j(x)}^*(x_j,t). \tag{5.2}$$

In the case of general meshes, the relation (5.2) replaces the initial formula (2.3), correct only for Bravais lattices, as illustrated in Fig. 13.

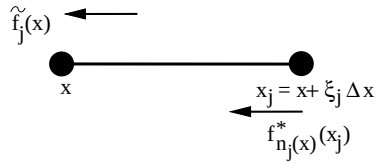

Figure 13: Iteration of a lattice Boltzmann scheme: the ingoing particles $\widetilde{f}_j(x)$ into vertex x are coming from the neighbouring vertex x_j after a relaxation step.

We precise now how to compare the ingoing particles $\widetilde{f}_j(x)$, the outgoing particles $f_j^*(x)$ emitted from the vertex x and the associated moments. We introduce first a matrix $\widetilde{M}(x)$ in order to compute the moments $m_k(x)$ from the ingoing particles. As previously (see the relation (2.5)), we suppose given a family $\mathcal{P}$ of polynomials p_k. In an analogous way suggested by the relation (2.6), we just reverse the direction of velocities and we have $\widetilde{M}(x)_{kj} = p_k(-\xi_j)$, with $p_k \in \mathcal{P}$. If the polynomials 1, X and Y are the first polynomials of the family $\mathcal{P}$, we have as in the previous studies $\widetilde{M}(x)_{0j} = 1$, $\widetilde{M}(x)_{\alpha j} = -\xi_j^\alpha(x)$, $1 \leq \alpha \leq d$. The moments are evaluated for the incoming particles with the natural relation

$$m_k(x) \equiv \sum_j \widetilde{M}(x)_{kj} \widetilde{f}_j(x), \quad 0 \leq k \leq q-1, \quad x \in \mathcal{L}. \tag{5.3}$$

The relaxation step is essentially unchanged. The moments can be seen as the eigenvectors of the jacobian of the relaxation matrix (see *e.g.* [11]) and this operator is diagonal with this representation:

$$m_k^*(x) = m_k(x) + s_k(x)\left(m_k^{\mathrm{eq}}(x) - m_k(x)\right), \tag{5.4}$$

where the index k in relation (5.4) is running on all nonconserved moments. The outgoing particles after relaxation are supposed to be a **linear** functional of the moments:

$$f_j^*(x) \equiv \sum_k P(x)_{jk} m_k^*(x), \quad 0 \leq j \leq q-1, \quad x \in \mathcal{L}. \tag{5.5}$$

The question is now to determine the matrix P. We have the following property.

Proposition 5.1 (Transition matrix from moments to particle distribution)**.** If the Taylor expansion approach is valid at the order zero and if each internal node of lattice $\mathcal{L}$ is of constant degree (the number of neighbours of each vertex does not depend of the vertex $x \in \mathcal{L}$), the matrix $P(x)$ of relation (5.5) is given by the relation

$$P(x)_{i\ell} = \left(\widetilde{M}(x_i)\right)^{-1}_{n_i(x)\,\ell}. \tag{5.6}$$

Proof. The proof can be conducted as follows. We start from the time iteration (2.3) of the lattice Boltzmann scheme. Then after multiplication by the matrix $\widetilde{M}(x)$, with the help of (5.3), (5.2) and (5.5), we have

$$\begin{aligned}
&m_k(x, t+\Delta t) \\
&= \sum_j \widetilde{M}(x)_{kj} \widetilde{f}_j(x, t+\Delta t) = \sum_j \widetilde{M}(x)_{kj} f^*_{n_j(x)}(x_j, t) \\
&= \sum_j \widetilde{M}(x)_{kj} \sum_\ell P(x_j)_{n_j(x)\ell} m_\ell^*(x_j, t) = \sum_\ell \Big(\sum_j \widetilde{M}(x)_{kj} P(x_j)_{n_j(x)\ell}\Big) m_\ell^*(x + \xi_j \Delta x, t).
\end{aligned}$$

We expand this relation at order one. Due to relaxation, we just have a small perturbation between m and m^*:

$$m_k(x)+\mathcal{O}(\Delta t)=m_k^*(x)+\mathcal{O}(\Delta x).$$

In consequence,

$$\sum_j \widetilde{M}(x)_{kj}\, P(x_j)_{n_j(x)\ell} \equiv \delta_{k\ell}$$

and in other terms,

$$P(x_j)_{n_j(x)\ell}=\big(\widetilde{M}(x)\big)^{-1}_{j\ell}.$$

We change the names of the vertices. We replace the letter x_j by the letter x. Then we replace the index $n_j(x)$ by some neighbor i of vertex x and the index j is now equal to $n_i(x)$. With this change of notation, we obtain $P(x)_{i\ell}=\big(\widetilde{M}(x_i)\big)^{-1}_{n_i(x)\ell}$ which is exactly the relation (5.6). □

We can now make explicit the d'Humières lattice Boltzmann scheme on an arbitrary mesh where the degree of each vertex is constant. When all the outgoing densities of particles $f_j^*(x,t)$ are known for all the vertices of the lattice at some discrete time t, the ingoing densities $\widetilde{f}_j(x,t+\Delta t)$ at the new time step are simply evaluated by a free flight (5.2) during one time step. Then the moments m_k are a local linear transform of the particle densities thanks to (5.3). The first moments compose a set $W(x)$ of conserved variables and the equilibrium moments $m^{\rm eq}$ are a given (in general nonlinear) function $G(W)$ of this field: $m_k^{\rm eq}(x)=G_k(W(x))$, $x\in\mathcal{L}$. The relaxation of moments follow the relation (5.4). Note that in general the coefficients $s_k(x)$ now depend *a priori* explicitly on the vertex x. Last but not least, the outgoing particles at the new time step from the vertex x follow the local linear transform (5.5).

6 D2T4 scheme for equilateral triangles

We consider a general two-dimensional mesh $\mathcal{L}$ composed by triangles. Note here that a cellular complex is composed by "vertices" in $\mathcal{L}^0$ of dimension zero, by edges in $\mathcal{L}^1$ of dimension one and by triangles of dimension two: $x\in\mathcal{L}^2$. In other words, we adopt a "cell center" framework in the sense proposed in Roache [33]. We can also locate the degree of freedom x at the center of gravity of the corresponding triangle. Remark that we make here *a priori* no other regularity hypothesis. Each triangle x has three edges. Each edge inside the border of x is part of the boundary of (at most) two triangles : the triangle x itself and its $j^{\rm th}$ neighbor x_j. It is then natural to consider outgoing particles $(f_j)_{0\leq j\leq 4}$ going from x towards x_j with a local velocity $\xi_j(x)\Delta t$ chosen in such a way that the centers of both triangles x and x_j are joined in exactly one time step of duration Δt. Of course, the null velocity is not excluded. This remark explains the name "D2T4" of this type of lattice Boltzmann scheme. A typical regular mesh for a D2T4 computation is presented in Fig. 14.

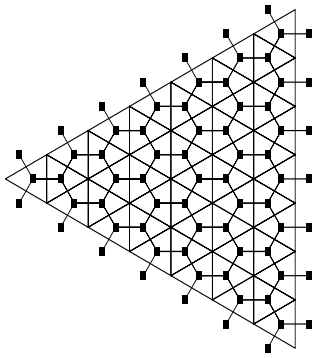

Figure 14: Typical mesh with equilateral triangles. The four degrees of freedom of D2T4 scheme are located at the center of gravity of each triangle. The links between triangles create the dual hexagonal mesh around the vertices of the triangular mesh.

The degrees of freedom in Fig. 14 are the centers of the initial triangular mesh. This "secondary mesh" is no longer a Bravais lattice. We lose the possibility of straight propagation of particles in the lattice and also the symmetry property of Bravais meshes emphasized in Fig. 1. But we keep the property that the number of neighbours is constant. And this property is maintained whatever the initial triangulation with cellular complexes.

We observe that such a lattice contains only two types of equilateral triangles: the "left" and "right"' triangles as displayed in Fig. 15. We precise now the choices we have done to construct our scheme. The family $\mathcal{P}$ of polynomials is simply composed by a restriction of (2.5) to the first four terms: $\mathcal{P}=\{1,X,Y,X^2+Y^2\}$. Because we have two generic triangles, we have two families of neighboring directions

$$\xi^{\rm left}=(-1,0),\Big(\frac{1}{2},-\frac{\sqrt{3}}{2}\Big),\Big(\frac{1}{2},\frac{\sqrt{3}}{2}\Big),\quad \xi^{\rm right}=(1,0),\Big(-\frac{1}{2},\frac{\sqrt{3}}{2}\Big),\Big(-\frac{1}{2},-\frac{\sqrt{3}}{2}\Big).$$

We observe also that due to the simple numbering of local edges (see Fig. 15), we have the simple relations $n_j(x)\equiv j$ and $\xi_j^{\rm left}+\xi_j^{\rm right}=0$. In this contribution, we consider only one conserved variable $\rho=m_0\equiv\sum_{j=0}^3 f_j$. The moments at equilibrium are simply chosen with $m_1^{\rm eq}=m_2^{\rm eq}=0$ and $m_3^{\rm eq}=a_3\rho$.

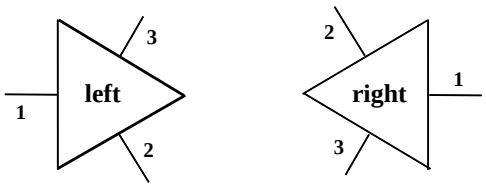

Figure 15: Two types of triangles for the D2T4 scheme with equilaterals. The local numbers are explicited for each edge.

Proposition 6.1 (Transition matrix for the D2T4 lattice Boltzmann scheme)**.** For the D2T4 lattice Boltzmann scheme defined previously, we have

$$P^{\text{left}} = \left(M^{\text{left}}\right)^{-1}, \qquad P^{\text{right}} = \left(M^{\text{right}}\right)^{-1}. \tag{6.1}$$

In this particular case, the relations (6.1) are exactly analogous to the ones for lattice Boltzmann schemes on Bravais lattices. In some sense, for the D2T4 scheme, the relations (6.1) remain (too!) simple!

Proof. Recall that due to (5.6), we have $P(x)_{i\ell} = \left(\widetilde{M}(x_i)\right)^{-1}_{n_i(x)\ell}$ with $n_i(x) \equiv i$ due to our precise choice of numbering (see Fig. 15). Then we have the two matrix equalities $P^{\text{left}}_{i\ell} = \left(\widetilde{M}^{\text{right}}\right)^{-1}_{i\ell}$ and $P^{\text{right}}_{i\ell} = \left(\widetilde{M}^{\text{left}}\right)^{-1}_{i\ell}$. We remark also that $M^{\text{left}}_{kj} = p_k(\xi^{\text{left}}_j)$ and $\widetilde{M}^{\text{left}}_{kj} = p_k(-\xi^{\text{left}}_j)$. Analogously $M^{\text{right}}_{kj} = p_k(\xi^{\text{right}}_j)$ and $\widetilde{M}^{\text{right}}_{kj} = p_k(-\xi^{\text{right}}_j)$. But $\xi^{\text{left}}_j + \xi^{\text{right}}_j = 0$, then $P^{\text{left}} = \left(\widetilde{M}^{\text{right}}\right)^{-1} = (M^{\text{left}})^{-1}$ and for the other family of triangles $P^{\text{right}} = \left(\widetilde{M}^{\text{left}}\right)^{-1} = (M^{\text{right}})^{-1}$. The relation (6.1) is established. □

Taylor expansion analysis for the D2T4 scheme

The analysis can now be conducted without difficulty in the same framework than previously. We adopt the diffusive-scaling (3.3). After some developments with the help of formal calculus (see *e.g.* [13]) we derive the equivalent partial differential equation at the order 6:

$$\begin{aligned}\frac{\partial \rho}{\partial t} - \mu \Delta \rho = \frac{a_3 \zeta}{24} (12\sigma_1^2 - 1) \Delta x \left(\partial_x^2 - 3\partial_y^2\right)\left(\partial_x \rho\right) + \Theta_2 \Delta x^2 \Delta^2 \rho \\ + \Theta_3 \Delta x^3 \left(\partial_x^2 - 3\partial_y^2\right) \Delta \left(\partial_x \rho\right) + \Delta x^4 A_6 \rho + \mathcal{O}(\Delta x^6).\end{aligned} \tag{6.2}$$

The notation σ_k is identical to the one used at Hénon's relation [19]. The diffusion coefficient μ satisfies the relation $\mu = \zeta a_3 \sigma_1$.

"First order", "second order", "third order" and "quartic" coefficients

We have chosen $\zeta = 1$. For first order simulations, we have taken the following numerical values

$$a_3 = 0.216506350946109, \quad s_1 = 1.2, \quad s_3 = 0.750796078775233 \tag{6.3}$$

compatible with a diffusion coefficient $\mu = 0.0721687836487032 = \frac{1}{4\sqrt{12}}$. With the choice $\sigma_1 = \frac{1}{\sqrt{12}}$ the scheme is at least second order accurate (see the right hand side of (6.2)) and we take parameters to fit the previous choice of the diffusion coefficient:

$$a_3 = 0.25, \quad s_1 = 1.267949192431122. \tag{6.4}$$

With the particular value

$$s_3 = 0.422649730810374, \tag{6.5}$$

we have $\Theta_2 \neq 0$ and the D2T4 scheme is formally second order accurate. With

$$s_3 = 0.758775495823486, \tag{6.6}$$

we have $\Theta_2 = 0$, $\Theta_3 \neq 0$ and the D2T4 scheme is formally third order accurate. With the choice of parameters

$$s_3 = 0.732050807568877 = \sqrt{3} - 1, \tag{6.7}$$

id est $\sigma_3 = \frac{\sqrt{3}}{2}$, we have $\Theta_2 = \Theta_3 = 0$. With these conditions, the D2T4 scheme is theoretically fourth order accurate.

7 Diffusion simulations with the D2T4 scheme

We have done essentially the same simulations as performed with the D2T7 lattice Boltzmann scheme (see Section 4).

One point periodic analysis

The results are presented in Fig. 16. The theoretical orders with the four choices of parameters proposed previously are exactly the one proposed by the Taylor expansion analysis. A defect of isotropy for the numerical diffusivity is clearly visible for parameters that lead to a first order and third order schemes with this D2T4 simulator.

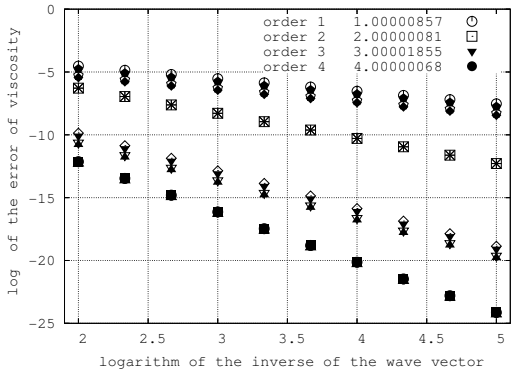

Figure 16: One point periodic analysis. Error $\epsilon \equiv |\mu - \mu_{\rm num}|$ between numerical and theoretical diffusivities. Four sets of parameters defined at relations (6.3), (6.4), (6.5), (6.6) and (6.7) lead to schemes of several orders. The measured orders with a linear regression are displayed in the right column.

Periodic pipe and rectangle

We have tested the fourth order version (6.4), (6.7) of the D2T4 lattice Boltzmann scheme on two simple periodic geometries presented in Section 4. The numerical results (Fig. 17) show that the scheme is convergent, but simply at second order accuracy.

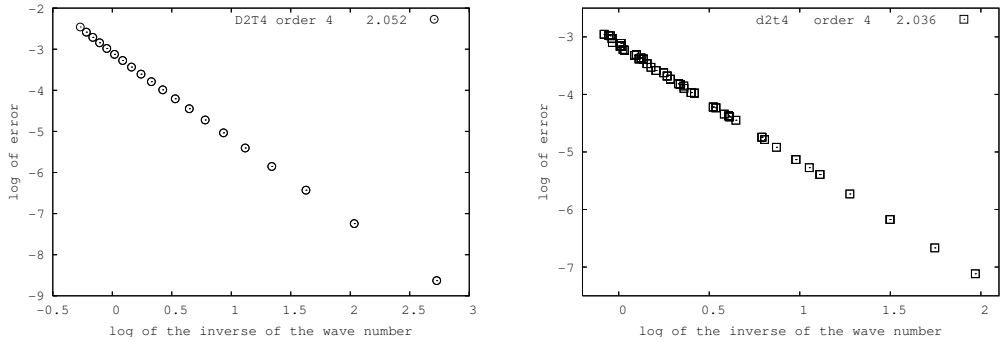

Figure 17: D2T4 lattice Boltzmann scheme for the heat equation. Periodic modes for a pipe with $nx=96$ and $ny=4$ mesh points (left) and a rectangle of $nx=36$ by $ny=52$ points (right). Error $\epsilon \equiv |\mu-\mu_{\rm num}|$ between exact and numerical diffusivities. The predicted coefficients for the order 4 define a second order scheme in this particular case.

Harmonic polynomials on a triangle

The numerical computation of Laplace equation with non-homogeneous boundary conditions has been also performed by integrating the heat equation and taking the limit for time large enough. Our simulation (Fig. 18) shows that the D2T4 scheme is convergent with second order accuracy. Nevertheless the second order and fourth order versions of the scheme give essentially the same results.

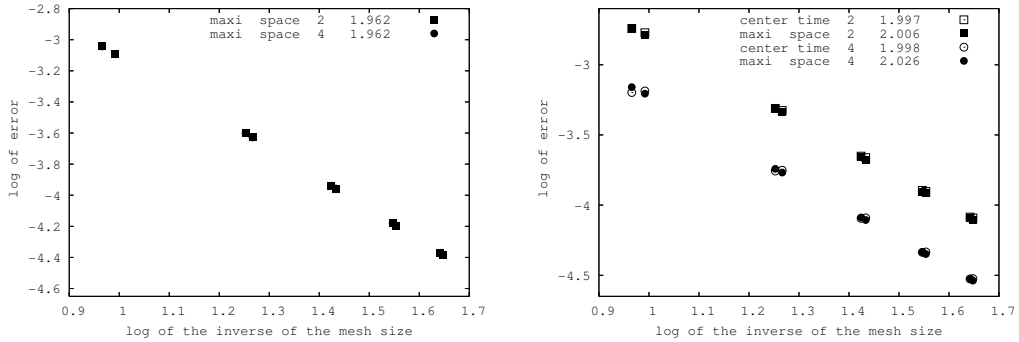

Figure 18: Two-dimensional computation of the harmonic function $p_H(x,y)=x^2-y^2$ on a triangle with the D2T4 lattice Boltzmann scheme (left). Convergence of the L^∞ error for several meshes. The D2T4 lattice Boltzmann scheme remains of order 2 even if quartic parameters are used in the simulation. Dissipation of the first Dirichlet mode for an equilateral triangle (right). Time and L^∞ space errors for several meshes and several "orders". The numerical accuracy is equal to 2 for all the parameters. With "quartic" parameters the absolute level of the error is substantially reduced.

Dissipation of a triangular Dirichlet mode

The dissipation of the first mode described at Fig. 7 for the D2T7 scheme has been constructed without difficulty. Now the two main versions of the scheme (second and fourth

orders) converge with second order accuracy as shown in Fig. 18. We observe that even if no extra order of convergence has been obtained, the results with quartic parameters give a better precision.

Dirichlet modes for a triangle

The simulations done with the D2T7 lattice Boltzmann scheme have been compared with a D2T4 simulator. The results (Fig. 19) explicit this comparison. A first result is that the level of error for D2T4 is comparable with D2T7 results at order two. If we look precisely to the error fields, distinguished contribution is due to the boundary conditions.

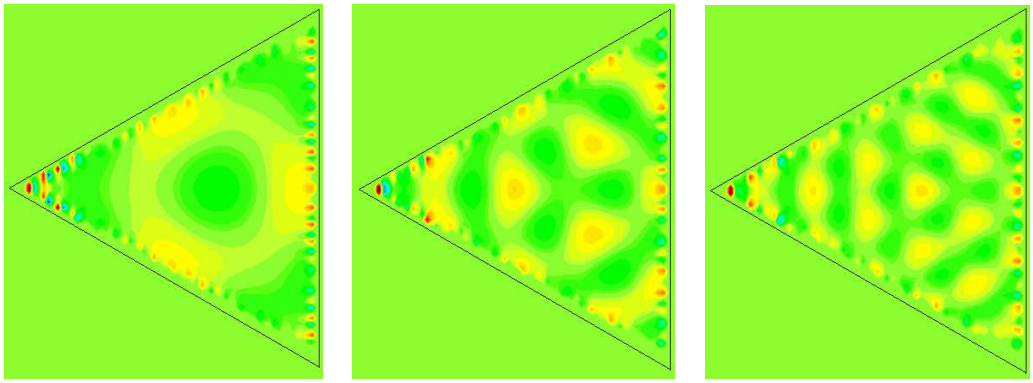

Figure 19: Isovalues of the errors for D2T4 computation of Dirichlet modes of an equilateral triangle. The exact reference eigenvalues are equal respectively to 12, 48 and 108 and the computed ones to 11.97493, 47.59816 and 105.95870. This figure can be compared to second order accurate D2T7 results at Figs. 9, 10 and 11 respectively.

8 Conclusion

We have proposed an extension of the lattice Boltzmann method for triangular meshes. Our first step concerns a single conservation law and we made numerical simulations for the heat equation. For an extension of the discrete particle method, we have considered non Bravais lattices such that the degree of each vertex is constant. Our formulation does not need any finite volume or Delaunay-Voronoi triangulation hypothesis as in the previous contributions. We have used the Taylor expansion analysis with a diffusive scaling to explicit some parameters of the d'Humières scheme. With this method, it is possible to get formally a better accuracy. Our simulations show that this extra accuracy can be obtained with very fundamental one point periodic hypothesis. In more realistic cases, this extra-accuracy is in general not observed.

We think that triangular meshes explicit the limit of validity of the Taylor expansion analysis. In fact when we write the lattice Boltzmann scheme with the relation (2.3) or (5.2) and when we perform the Taylor expansion, we suppose that there exists a very

regular function $f(x,t)$ of space and time that support the definition of the scheme. In particular, this function is supposed to be independent of the lattice! This last Ansatz is in defect for triangular meshes on nonsymmetric lattices as D2T4. Note that this kind of remark recover other critics [4, 17] relative to this kind of symptotic analysis [25, 42].

Two directions of research are natural in the continuation of the present contribution. First we can try to develop a true mathematical analysis of the lattice Boltzmann scheme, following *e.g.* previous work of Junk and Yong [21] with appropriate mathematical tools, as done typically by Ciarlet and Raviart for finite elements [7] or Gallouët and coworkers for finite volumes [6]. Second we can extend triangular lattice Boltzmann schemes to systems with other conservation laws for acoustics and fluid flow applications, revisiting the breakthrough of Frisch, Hasslacher and Pomeau [14]. Preliminary results have been obtained for D2T10, which are not described in this article due to unnecessary complications.

Acknowledgments

The authors thank the "LaBS project" (Lattice Boltzmann Solver, www.labs-project.org), funded by the French "FUI8 research program", for supporting this contribution. Last but not least, the authors thank the referees for very constructive remarks. Some of them have been incorporated into the present edition of the article.

References

[1] W.E. Arnoldi. The principle of minimized iteration in the solution of the matrix eigenvalue problem, Quarterly of Applied Mathematics, vol. 9, pp. 17-25, 1951. See the "Arpack" software at `http://www.caam.rice.edu/software/ARPACK`.

[2] J.T. Beale, A. Majda. Vortex methods I: Convergence in three dimensions, Vortex methods II: Higher order accuracy in two and three dimensions, Mathematics of Computation, vol. 39, pp. 1-27 and 29-52, 1982.

[3] M. Bouzidi, M. Firdaouss, P. Lallemand. Momentum transfer of a Boltzmann-lattice fluid with boundaries, Physics of Fluids, vol. 13, n° 11, pp. 3452-3459, 2001.

[4] S.C. Chang. A critical analysis of the modified equation technique of Warming and Hyett, Journal of Computational Physics, vol. 86, pp. 107-126, 1990.

[5] H. Chen. Volumetric formulation of the lattice Boltzmann method for fluid dynamics: Basic concept, Physical Review E, vol. 58, pp. 3955-3963, 1998.

[6] S. Champier, T. Gallouët, R. Herbin. Convergence of an Upstream Finite Volume Scheme for a Nonlinear Hyperbolic Equation on a Triangular Mesh, Numerische Mathematik, vol. 66, pp. 139-157, 1993.

[7] P.G. Ciarlet, P.A. Raviart. General Lagrange and Hermite interpolation in $\mathbb{R}^n$ with applications to finite element methods, Archive for Rational Mechanics and Analysis, vol. 46, pp. 177-199, 1972.

[8] G.H. Cottet, S. Mas-Gallic. A particle method to solve the Navier-Stokes system, Numerische Mathematik, vol. 57, pp. 805-827, 1990.

[9] D. d'Humières. Generalized Lattice-Boltzmann Equations, in Rarefied Gas Dynamics: Theory and Simulations, vol. 159 of AIAA Progress in Aeronautics and Astronautics, pp. 450-458, 1992.
[10] F. Dubois. Equivalent partial differential equations of a lattice Boltzmann scheme, Computers and Mathematics with Applications, vol. 55, pp. 1441-1449, 2008.
[11] F. Dubois. Introduction au Schéma de Boltzmann sur Réseau, Master degree Lectures given at Université Paris-Sud, winter 2009-2010, unpublished. See `http://www.math.u-psud.fr/~fdubois/cours/lbs-2010.html`.
[12] F. Dubois, P. Lallemand. On lattice Boltzmann scheme, finite volumes and boundary conditions, Progress in Computational Fluid Dynamics, vol. 8, pp. 11-24, DOI: 10.1504/PCFD.2008.018075, 2008.
[13] F. Dubois, P. Lallemand. Towards higher order lattice Boltzmann schemes, Journal of Statistical Mechanics: Theory and Experiment, P06006, doi: 10.1088/1742-5468/2009/06/P06006, 2009.
[14] U. Frisch, B. Hasslacher, Y. Pomeau, Lattice gas automata for the Navier Stokes equation, Physical Review Letters, vol. 56, n^o 14, pp. 1505-1508, 1986.
[15] P.L. George. Automatic Mesh Generation: Applications to Finite Element Methods, John Wiley & Sons, Inc. New York, USA, 1992.
[16] I. Ginzburg, F. Verhaeghe, D. d'Humières. Two-relaxation-time lattice Boltzmann scheme: about parametrization, velocity, pressure and mixed boundary conditions, Communications in Computational Physics, vol. 3, pp. 427-478, 2008.
[17] D. Griffiths, J. Sanz-Serna. On the scope of the method of modified equations, SIAM Journal on Scientific and Statistical Computing, vol. 7, pp. 994-1008, 1986.
[18] F.H. Harlow, M.A. Ellington, J.H. Reid. The particle-in-cell computing method for fluid dynamics, Methods in Computational Physics, vol. 3, (B. Alder, S. Fernbach, M. Rotenberg Eds), pp. 319-343, Academic Press, New York, 1964.
[19] M. Hénon. Viscosity of a Lattice Gas, Complex Systems, vol. 1, pp. 763-789, 1987.
[20] M. Junk, A. Klar, L.S. Luo. Asymptotic analysis of the lattice Boltzmann equation, Journal of Computational Physics, vol. 120, pp. 676-704, 2005.
[21] M. Junk, W.A. Yong. Weighted L^2-Stability of the Lattice Boltzmann Method, SIAM Journal on Numerical Analysis, vol. 47, pp. 1651, 2009.
[22] I.V. Karlin, S. Succi, S. Orszag. Lattice Boltzmann Method for Irregular Grids, Physical Review Letters, vol. 82, pp. 5245-5248, 1999.
[23] A. Klales, D. Cianci, Z. Needell, D.A. Meyer, P.J. Love. Lattice gas simulations of dynamical geometry in two dimensions, Physical Review E, vol. 82, pp. 046705, 2010.
[24] P. Lallemand, L.S. Luo. Theory of the lattice Boltzmann method: Dispersion, dissipation, isotropy, Galilean invariance, and stability, Physical Review E, vol. 61, pp. 6546-6562, June 2000.
[25] A. Lerat, R. Peyret. Noncentered Schemes and Shock Propagation Problems, Computers and Fluids, vol. 2, pp. 35-52, 1974.
[26] P.J. Love, D. Cianci. From the Boltzmann equation to fluid mechanics on a manifold, Philosophical Transactions of the Royal Society A, vol. 369, pp. 2362-2370, 2011.
[27] B.J. McCartin. Eigenstructure of the Equilateral Triangle, Part I: The Dirichlet Problem, SIAM Review, vol. 45, pp. 267-287, 2003.
[28] S. Mas Gallic, P.A. Raviart. A Particle Method for First order Symmetric Systems, Numerische Mathematik, vol. 51, pp. 323-352, 1987.
[29] G. Peng, H. Xi, C. Duncan, S. H. Chou. A Finite Volume Scheme for the Lattice Boltzmann

Method on Unstructured Meshes, Physical Review E, vol. 59, pp. 4675-4682, 1999.
[30] G. Pontrelli, S. Ubertini, S. Succi. The unstructured lattice Boltzmann method for non-Newtonian flows, Journal of Statistical Mechanics: Theory and Experiment, P06005, doi: 10.1088/1742-5468/2009/06/P06005, 2009.
[31] Y. Qian, D. d'Humières, P. Lallemand, Lattice BGK Models for Navier-Stokes Equation, Europhysics Letters, vol. 17, pp. 479-484, 1992.
[32] P.A. Raviart. An analysis of particle method, in Numerical Methods in Fluid Mechanics (F. Brezzi Ed.), Lecture Notes in Mathematics, vol. 1127, pp. 243-324, Springer Verlag, 1985.
[33] P.J. Roache. Computational Fluid Dynamics, Hermosa Publishers, Albuquerque, 1972.
[34] Y. Sone. Asymptotic theory of flow of rarefied gas over a smooth boundary I, in Rarefied Gas Dynamics, L. Trilling and H.Y. Wachmann Eds, Academic press, New York, pp. 243-253, 1969.
[35] S. Ubertini, G. Bella, S. Succi. Lattice Boltzmann method on unstructured grids: Further developments, Physical Review E, vol. 68, 016701, 2003.
[36] S. Ubertini, S. Succi, G. Bella. Lattice Boltzmann schemes without coordinates, Philosophical Transactions of the Royal Society A, vol. 362, pp. 1763-1771, 2004.
[37] R.G.M. van der Sman, M.H. Ernst. Diffusion Lattice Boltzmann scheme on an Orthorhombic Lattice, Journal of Statistical Physics, vol. 94, pp. 203-217, 1999.
[38] R.G.M. van der Sman, M.H. Ernst. Convection-Diffusion Lattice Boltzmann scheme for Irregular Lattices, Journal of Computational Physics, vol. 160, pp. 1-17, 2000.
[39] R.G.M. van der Sman. Lattice Boltzmann scheme for Diffusion on Triangular Grids, P.M.A. Sloot et al. (Eds), Lecture Notes in Computational Science, vol. 2657, pp. 1072-1081, Springer-Verlag Berlin, Heidelberg, 2003
[40] R.G.M. van der Sman. Diffusion on unstructured triangular grids using Lattice Boltzmann, Future Generation Computer Systems, vol. 20, pp. 965-971, 2004.
[41] G. Vijayasundaram. Transonic flow simulations using an upstream centered scheme of Godunov in finite elements, Journal of Computational Physics, vol. 63, pp. 416-433, 1986.
[42] R.F. Warming, B.J. Hyett. The modified equation approach to the stability and accuracy analysis of finite difference methods, Journal of Computational Physics, vol. 14, pp. 159-179, 1974.